A chemical inhibitor of heat shock protein 78 (HSP78) from *Leishmania donovani* represents a potential antileishmanial drug candidate

Received for publication, May 27, 2020, and in revised form, May 28, 2020 Published, Papers in Press, May 29, 2020, DOI 10.1074/jbc.RA120.014587

Sonali Das[1,‡], Anindyajit Banerjee[2,‡], Mohd Kamran[1], Sarfaraz Ahmad Ejazi[1], Mohammad Asad[1], Nahid Ali[1,*], and Saikat Chakrabarti[2,*]

From the [1]Infectious Diseases and Immunology Division, CSIR-Indian Institute of Chemical Biology, Jadavpur, Kolkata, West Bengal, India and the [2]Structural Biology and Bioinformatics Division, CSIR-Indian Institute of Chemical Biology, Salt Lake, Kolkata, West Bengal, India

Edited by Ursula Jakob

The emergence of resistance to available antileishmanial drugs advocates identification of new drug targets and their inhibitors for visceral leishmaniasis. Here, we identified *Leishmania donovani* heat shock protein 78 (LdHSP78), a putative caseinolytic protease, as important for parasite infection of host macrophages and a potential therapeutic target. Enrichment of LdHSP78 in infected humans, hamsters, and parasite amastigotes suggested its importance for disease persistence. Heterozygous knockouts of *L. donovani* HSP78 (*LdHSP78+/−*) and *Leishmania mexicana* HSP78 (*LmxHSP78+/−*) were generated using a flanking UTR-based multifragment ligation strategy and the CRISPR-Cas9 technique, respectively to investigate the significance of HSP78 for disease manifestation. The *LdHSP78+/−* parasite burden was dramatically reduced in both murine bone marrow-derived macrophages and hamsters, in association with enrichment of proinflammatory cytokines and NO. This finding implies that *LdHSP78+/−* parasites cannot suppress immune activation and escape NO-mediated toxicity in macrophages. Furthermore, phosphorylation of the mitogen-activated protein kinase p38 was enhanced and phosphorylation of extracellular signal-regulated kinase 1/2 was decreased in cells infected with *LdHSP78+/−* parasites, compared with WT parasites. Virulence of the *LdHSP78+/−* strain was restored by episomal addition of the *LdHSP78* gene. Finally, using high-throughput virtual screening, we identified P^1,P^5-di(adenosine-5′)-pentaphosphate (Ap5A) ammonium salt as an LdHSP78 inhibitor. It selectively induced amastigote death at doses similar to amphotericin B doses, while exhibiting much less cytotoxicity to healthy macrophages than amphotericin B. In summary, using both a genetic knockout approach and pharmacological inhibition, we establish LdHSP78 as a drug target and Ap5A as a potential lead for improved antileishmanial agents.

Under general as well as inducible environmental stresses, organisms respond by synthesizing a group of chaperons called heat shock proteins (HSPs) (1). HSPs facilitate survivability of organisms by assisting in maturation, activation, translocation, and degradation of misfolded nascent proteins (1). Interestingly, for some pathogens like *Leishmania donovani*, which have a digenetic life cycle, inducible heat stress is a vital part of their biology. They are transmitted from the poikilothermic sand fly gut to the homeothermic mammalian macrophage, which involves a shift in temperature of almost 10 °C. This temperature upshift is a key trigger for the differentiation of *Leishmania donovani* promastigotes (sand fly stage) to amastigotes (mammalian stage) (2). Heat stress unleashed by the macrophage leads to enrichment of various *Leishmania* HSPs, which determine the pathology of the disease. In cutaneous leishmaniasis, *Leishmania major* can tolerate heat shock up to 35 °C, which results in tropical skin lesions; in visceral leishmaniasis (VL), *L. donovani* can sustain temperatures as high as 37–40 °C, which correlates with visceralization of the parasites (3). Besides management of heat stress, protozoan HSPs play a substantial role in virulence. A recent transcriptomic analysis revealed a positive correlation between the *Plasmodium* HSPs and regulatory interleukin levels in patients with malignant malaria (4).

In other organisms, HSPs belonging to the caseinolytic protease B (ClpB) group, like bacterial ClpB (*Escherichia coli*), yeast (*Saccharomyces cerevisiae*) HSP104, and plant HSP101, have extraordinary capacity to rescue disaggregated proteins during severe heat stress, which is otherwise lethal for the organisms (5, 6). To date, functional study of only one ClpB protein, HSP100 (LmxHSP100), has been reported in *Leishmania* biology (6). It has been shown that heat-stressed parasites are strongly enriched with LmxHSP100, and *LmxHSP100−/−* null mutants of *L. major* are unable to establish infection within murine peritoneal macrophages, as well as BALB/c mice (6). *LdHSP100−/−* null mutants of *L. donovani* showed impaired amastigote development, and LdHSP100 is also found to be involved in the transport of exosome-mediated virulence factors during infection (6).

A major global challenge for antileishmanial therapy is overcoming chemoresistant and treatment failure cases arising from treatment with the classical antileishmanial agents available on the market, such as antimonial salts, amphotericin B (AmB), miltefosine, and paromomycin (7, 8). Most of these

This article contains supporting information.

‡These authors contributed equally to this work.
*For correspondence: Saikat Chakrabarti, saikat@iicb.res.in; Nahid Ali, nali@iicb.res.in.
Present address for Anindyajit Banerjee: Tata Translation Cancer Research Center, Tata Medical Center, Kolkata, West Bengal, India.
Present address for Mohammad Asad: Dept. of Medicine, Albert Einstein College of Medicine, Bronx, New York, USA.

drugs are repurposed and non-target based. Recent studies have highlighted protozoan HSPs, such as HSP90 in *Plasmodium falciparum* and *Trypanosoma evansi*, as potential drug targets. These factors prompted us to explore the role of LdHSP78 (UniProt code LdBPK_020680), a putative member of the ClpB protease family, as a potential drug target in *L. donovani* infection.

A BLAST search revealed that LdHSP78 expresses a 78-kDa protein orthologous to LmjF27.2630 of *L. major* and Tb927.2.3030 of *Trypanosoma brucei* (6, 9). Significant sequence structural similarity has been observed between LdHSP78 and a ClpB protein from *Thermus thermophilus* that is composed of an N-terminal domain, two nucleotide-binding domains (NBDs) (NBD1 and NBD2), and a middle coiled coil domain (MD region) (10, 11). Here, we propose the probable prominence of LdHSP78 for VL progression. The importance of HSP78 for survival of the parasites was assessed by *HSP78* knockout generation in *L. donovani* (*LdHSP78*+/−) and *Leishmania mexicana* (*LmxHSP78*+/−), with the virulence phenotype of *LdHSP78*+/− parasites being rescued by episomal overexpression of *LdHSP78* (resKO). However, the lethality of null mutants (*Ld/LmxHSP78*−/−) and successful conditional knockout of *LdHSP78* generation suggested probable essentiality of the gene for *Leishmania*, but more experimental validations are awaited. Infectivity and the capacity to suppress the antileishmanial immune responses activated by host macrophages were determined by infecting murine bone marrow-derived macrophages (BMDMs) and Syrian golden hamsters with WT, *LdHSP78*+/−, and resKO parasites. Furthermore, P^1,P^5-di(adenosine-5′)-pentaphosphate (Ap_5A) ammonium salt, a synthetic ATP analog, was identified as a pharmacological inhibitor of LdHSP78 protein. The antileishmanial efficacy of Ap5A was evaluated and compared with that of the generic antileishmanial drug AmB in healthy BMDMs, promastigotes, and amastigotes. Notably, Ap5A induced much less collateral damage to host cells, unlike AmB. Hence, our study reveals LdHSP78 as a potential antileishmanial therapeutic target while identifying its inhibitor, Ap5A, as a promising lead molecule against VL.

Results

LdHSP78 is a stress-regulating protein that is enriched during VL

LdHSP78 is a putative ATP-dependent Clp subunit-containing protein (UniProt code LdBPK_020680). It is encoded by a single exon located at *L. donovani* chromosome 2 and is highly conserved throughout the *Leishmania* spp. while being nonorthologous to human proteins (no human orthologs with >20% sequence identity are available). Involvement of HSP78 in VL was initially perceived from semiquantitative PCR of *LdHSP78* transcripts from *L. donovani*-infected BMDMs (Fig. 1*A*). Moreover, enrichment of the same was detected in the peripheral blood, spleen, and liver of 3-month-infected golden Syrian hamsters (Fig. 1*B*). A study conducted with a small cohort of VL patient blood samples correlated with the mRNA expression profile of animals (Fig. 1*B*). To establish chaperone-like properties of LdHSP78, we mimicked the host phagosomal microenvironment by growing *L. donovani* promastigotes in M199 (pH 4.0 and pH 5.5) at 37 °C under axenic conditions. Almost 40–55-fold higher expression of *LdHSP78* mRNA was obtained at pH 5.5 and 37 °C, compared with that obtained at pH 7.0 and 22 °C (Fig. 1*C*). These data collectively indicated that HSP78 levels were higher not only during physiological stress of the parasites but also under VL conditions.

Generation of HSP78 transgenic cell lines

LdHSP78 knockout parasite cell lines were generated using both a flanking UTR-based multifragment ligation strategy (Fig. S1*A*) and the CRISPR-Cas9 technique (Fig. S1*N*). For UTR-mediated knockout generation, 5′ (997 bp) and 3′ (946 bp) flanking regions (UTRs) of *LdHSP78* were directionally cloned (Fig. S1, *A* and *B*) at both sides of the hygromycin (*HYG*) (3245 bp) and puromycin (*PUR*) (3005 bp) cassettes, using specialized primers that incorporated overhangs with unique SfiI digestion sites at each fragment end (Fig. S1, *D* and *E*). The PacI-digested linearized 5397-bp *HYG* construct was transfected in log-phase parasites for generation of heterozygous knockouts (Fig. S1*E*). A separate population of WT parasites was maintained as mock-transfected cells (transfected with empty vector). *LdHSP78-HYG* (*LdHSP78*+/−) cells were cultured in 50 μg/ml HYG-supplemented M199. Next, pure *LdHSP78*+/− clones were collected by isolating single colonies from the serially diluted *LdHSP78*+/− cells grown on HYG-supplemented M199 agar.

Genomic DNA was isolated from log-phase WT and *LdHSP78*+/− promastigotes, and PCR was performed using primers spanning the flanking region to the ORFs of *HSP78* and *HYG* (Table S1, primers 5–8). The presence of both HSP78 and *HYG* in genomic DNA of *LdHSP78*+/− parasites suggested successful partial replacement of one *LdHSP78* allele with the *HYG* cassette (Fig. 1*D*). The 5′ UTR (997 bp) and 3′ UTR (946 bp) flanking regions, which had been chosen for knockout generation, were scanned against all 36 chromosomes of *L. donovani*. Sequence identity and coverage match of 100% were obtained only at chromosome 2 loci flanking the *HSP78* gene (Fig. S1*H*), and no sequence overlap with other chromosomes was observed, confirming the least off-target effect and high efficacy of the flanking region-mediated deletion technique.

LdHSP78 was overexpressed in *LdHSP78*+/− cell lines (resKO cell lines) by cloning the episomal vector pXG-GFP(+) (generously provided by Stephen Beverly, Washington University) at the BamHI and EcoRV sites (Fig. S1, *I–L*). *L. donovani* is a diploid organism; therefore, to completely deplete *LdHSP78*, two drug cassettes (*HYG* and *PUR*) were transfected successively. PacI-digested linearized 5397-bp *HYG* (Fig. S1*E*) and 4974-bp *PAC* (Fig. S1*F*) cassettes were serially transfected in log-phase parasites for generation of null mutants. Attempts were made to culture *LdHSP78-HYG/PAC* (*LdHSP78*−/−) cells in 50 μg/ml *HYG*- and 20 μg/ml *PUR*-supplemented medium. However, live parasite counts confirmed that null mutants started dying with days of culturing. Our multiple attempts to obtain live parasites from *HYG*- and *PUR*-supplemented M199

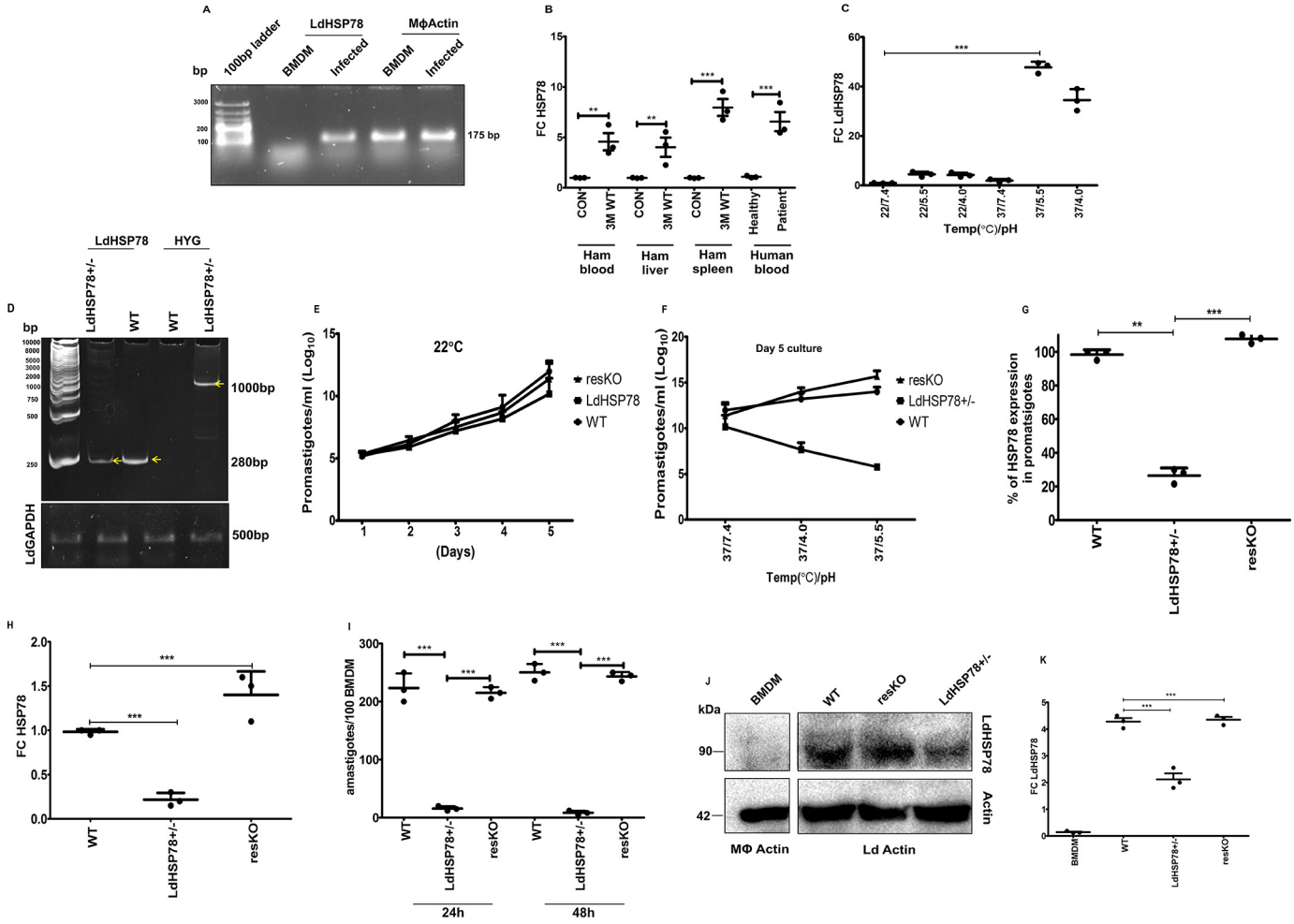

Figure 1. LdHSP78 is an essential chaperone for infection. *A*, semiquantitative PCR of *LdHSP78* mRNA in *L. donovani*-infected BMDMs. *B*, RT-PCR of *LdHSP78* mRNA from 3-month-infected hamster (*Ham*) spleen, liver, and blood and VL patient peripheral blood. The C_t value of *LdHSP78* was normalized against that of *L. donovani GAPDH* and plotted as fold change (*FC*) ($2^{-\Delta\Delta Ct}$). *C*, RT-PCR of LdHSP78 mRNA from promastigotes cultured at different temperature and pH values. The C_t value of *LdHSP78* was normalized against that of *L. donovani GAPDH* and plotted as fold change (*FC*) ($2^{-\Delta\Delta Ct}$). *D*, partial deletion of *LdHSP78* validation by urea-PAGE-based separation of PCR products, amplified from WT (control transfected) and *LdHSP78+/−* parasites (*L. donovani* actin is the loading control). *E* and *F*, Determination of *LdHSP78+/−* promastigote fitness under (*E*) normal conditions (22 ℃ and pH 7.4) and (*F*) amastigote-like conditions (37 ℃ and pH 4.0, 5.5, and 7.4). Growth kinetics of promastigotes were determined from 5-day cultures (to obtain maximum growth). *G* and *H*, RT-PCR-based determination of *LdHSP78* mRNA loads of WT, *LdHSP78+/−*, and resKO promastigotes (*G*) and amastigotes (*H*) in infected BMDMs. *I*, Giemsa staining of BMDMs infected with WT, *LdHSP78+/−*, and resKO parasites for 24 and 48 h at a 1:10 ratio. *J* and *K*, Western blotting of lysates from uninfected BMDMs (negative control) and WT, *LdHSP78+/−*, and resKO promastigotes (loading controls were macrophage actin and *L. donovani* actin). Fold changes of LdHSP78 were calculated from densitometric values of the bands. Each group is represented by three samples, and each experiment was performed in triplicate. Statistical significance (**, $p < 0.01$; ***, $p < 0.001$) was calculated using one-way analysis of variance followed by Dunnett's multiple-comparison test and unpaired two-tailed *t* test followed by Welch correction (each *dot* is representative of a single sample; $n = 3$ samples per group). Data represent mean ± S.D. (GraphPad Prism v5.0).

medium failed probably due to the essential nature of the *LdHSP78* gene for the promastigotes.

Parasites bearing an extrachromosomal copy of genes generally allow deletion of the chromosomal copies of essential genes. Therefore, promastigotes were transfected with the *pXG-HSP78* episome (pXG-GFP-HSP78-Neo+) to maintain an extra copy of genes, followed by double deletion of the chromosomal copies using *HYG* and *PUR* cassettes. The conditional knockout (cond KO- *LdHSP78−/−epiHSP78*) cells were maintained in the presence of *HYG*, neomycin (*NEO*), and *PUR* drug selection medium for 15 days, followed by depletion of *NEO* from the medium. Interestingly, we found that, despite *NEO* selection withdrawal (required for *pXG-HSP78* maintenance), cells still grew well and, following 7 days of culture, we isolated genomic DNA. *LdHSP78, HYG, NEO*, and *PUR* drug cassettes were PCR amplified. For amplification of *HSP78* and *NEO* genes, primers were designed against their respective ORF regions; for *HYG* and *PUR* cassettes, amplification primers spanning the 5′ flanking region of the *HSP78* gene and the respective drug ORF regions were designed (Table S1, primers 43–50). PCR data indicated that, in the absence of episomal *NEO*, *LdHSP78−/−* cells are holding back the extrachromosomal copy of *LdHSP78* for their survival (Fig. S1*M*).

We also attempted to design null mutants of *LmxHSP78* using the CRISPR-Cas9 system (*in silico* analysis showed >98% sequence homology of *LdHSP78* to *LmHSP78*) in Cas9-positive *L. mexicana* cell lines (generously provided by Jeremy Mottram's laboratory) (Fig. S1*N*), which indicated that a *HSP78* null mutation is probably lethal in *L. mexicana*. In this model also, only heterozygous parasites survived in the presence of

blasticidin (50 μg/ml) (Fig. S1*O*). Genomic DNA PCR showed successful replacement of one *LmHSP78* allele with the blasticidin cassette (Fig. S1*P*). Western blot analysis depicted significant reduction of *LmHSP78* in heterozygous cell lines, compared with WT cell lines (Fig. S1*Q*). These findings indicated that HSP78 might be essential for survival of the parasite, although more experimental validations are required to confirm this.

LdHSP78 is an essential chaperon for infection persistence in BMDMs

Chaperone-like activity of HSP78 was already indicated from its enrichment during pH and heat stress in *L. donovani* promastigotes (Fig. 1*C*). Physical fitness of WT, *LdHSP78+/−*, and resKO promastigotes was studied initially at 22 ℃, which indicated equivalent growth rates for all three cell lines at day 5 (Fig. 1*E*). Subsequently, it was found that, at pH 5.5 and 37 ℃, the growth rate of *LdHSP78+/−* parasites was reduced significantly, denoting the role of HSP78 in pH and heat stress management (Fig. 1*F*). Quantitative expression of *LdHSP78* mRNA obtained from promastigotes indicated ∼80% reduction of the mRNA in *LdHSP78+/−* promastigotes and almost 95% restoration of mRNA in resKO promastigotes (Fig. 1*G*). Analysis of *LdHSP78* mRNA levels from BMDMs infected with WT, *LdHSP78+/−*, and resKO parasites also depicted a similar profile of *LdHSP78* transcripts in *LdHSP78+/−* amastigotes (Fig. 1*H*). This was accompanied by a significant drop in the parasite burden at 24 h and 48 h postinfection in *LdHSP78+/−* parasite-infected BMDMs (Fig. 1*I*). We successfully reestablished the virulence of *LdHSP78+/−* parasites by episomal overexpression of *LdHSP78*. Complete restoration of *LdHSP78* mRNA was found in resKO parasite-infected BMDMs (Fig. 1*H*). Investigation of the infection index of resKO parasites in BMDMs also corroborated with mRNA data, establishing the significance of LdHSP78 for infection *in vitro* (Fig. 1*I*).

Protein level validation showed depletion of LdHSP78 in heterozygous cell lines

The most immunodominant peptide (127 amino acids; indicated in *purple* in Fig. S2*A*) of LdHSP78 was codon optimized and subcloned from pGEX-6P.1-Amp+ to the pET41a-Kan+ vector (Fig. S2, *B–D*). The hydrophobicity of the peptide was analyzed using a hydropathy plot, which indicated that the peptide sequence chosen is enriched with hydrophilic amino acids and ideal as a B-cell epitope (Fig. S2*E*). The epitope was then overexpressed and purified in the native form using nickel-nitrilotriacetic acid resin, and BALB/c mice were immunized with it (Fig. S2, *F–H*). Sera collected after three boosters were used for immunoblotting of the purified epitope, to analyze the quality of the generated antibody (Fig. S2*I*). Thereafter, partial depletion of *LdHSP78* and *LmHSP78* (previously mentioned) was validated by Western blotting from parasite lysates obtained from promastigote cell lines generated using flanking UTR-mediated and CRISPR-Cas9–mediated knockout technologies, respectively. Almost 50% or more depletion of HSP78 protein was obtained in *LmHSP78* (Fig. S2*Q*) and *LdHSP78+/−*, while complete restoration of LdHSP78 protein was achieved in resKO parasites (Fig. 1, *J* and *K*). The specificity of anti-HSP78 antibody was cross-validated using BMDM lysate, and no immunoreactive band was obtained (Fig. 1, *J* and *K*).

Down-regulation of proinflammatory cytokine synthesis during LdHSP78+/− infection in BMDMs

One of the major issues with antileishmanial therapy is overcoming immunosuppression induced by parasites. Our next question was whether partial depletion of *LdHSP78* would result in inability of parasites to overcome host immune activation. Significant down-regulation of proinflammatory cytokines and up-regulation of anti-inflammatory cytokines were observed in WT parasite-infected BMDMs. In contrast, in *LdHSP78+/−* parasite-infected macrophages, mRNA and protein levels of anti-inflammatory cytokines, such as transforming growth factor β (TGFβ) (Fig. 2, *A* and *E*), IL10 (Fig. 2, *B* and *F*), and IL27A (Fig. 2, *C* and *G*), were significantly depleted, whereas IL12A (Fig. 2, *D* and *H*) was significantly enriched. Thus, cytokine profiling revealed that proinflammatory cytokines were significantly inhibited during *LdHSP78+/−* parasite infection.

MAPK activation and NO generation instigated LdHSP78+/− parasite clearance from BMDMs

Extracellular signal-regulated kinase 1/2 (ERK1/2) and p38 mitogen-activated protein kinase (MAPK) are the two major MAPKs that are involved in the regulation of cytokine profiles and NO synthesis (12). These MAPKs require phosphorylation at their specific amino acids for their activation. Infection with WT parasites induced significant up-regulation of phospho-ERK1/2 (p-p44/p42, Thr202/Tyr204) (Fig. 3, *A* and *E*) and decreased levels of phospho-p38 (Thr180/Tyr182) (Fig. 3, *B* and *F*), while total MAPK expression levels remain constant. In contrast, reverse activation profiles of these proteins were found in *LdHSP78+/−* parasite-infected macrophages (Fig. 3).

Phosphorylation of ERK1/2 leads to enrichment of arginase 1 levels, which helps in parasite survival, whereas phospho-p38 MAPK leads to enrichment of inducible NOS (iNOS) expression, which mediates clearance of parasites by generation of NO (13). Therefore, we examined the levels of iNOS and arginase 1 expression, which suggested that *LdHSP78+/−* parasites were unable to exhaust iNOS and to enhance arginase 1 expression (Fig. 3, *C*, *D*, *G*, and *H*). Significant amounts of NO generation were obtained from BMDMs infected with the mutant parasites, compared with the WT ones (Fig. 3*I*). After overexpression of *LdHSP78* in resKO parasites, the immunosuppressive nature of parasites was significantly restored, with concomitant suppression of phospho-p38, iNOS and NO generation.

Partial loss of HSP78 affects the infectivity index of parasites in an in vivo experimental infection model

Golden Syrian hamsters are a well-established model that successfully mimics the pathophysiology of human VL infection (14, 15). Before infecting animals, the percentages of infective metacyclic promastigotes were determined in all of the parasite cultures by lipophosphoglycan-independent Ficoll density

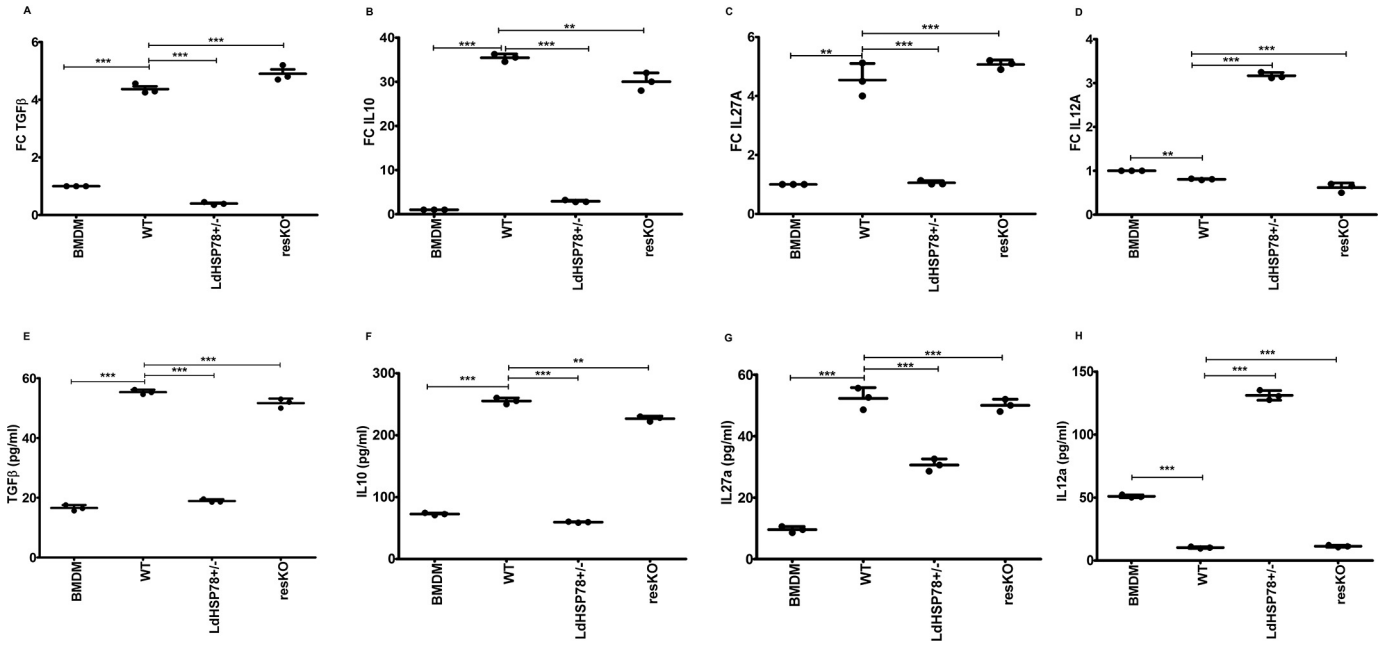

Figure 2. Cytokine profiling of BMDMs infected with LdHSP78-depleted and -overexpressing parasites indicated sustained proinflammatory cytokine responses. RT-PCR (*A–D*) and sandwich ELISAs (*E–H*) of proinflammatory (IL12A) and anti-inflammatory (IL10, IL27A, and TGFβ) cytokines from WT, *LdHSP78+/−*, and resKO parasite-infected BMDMs. Eight hours after infection, total RNA was isolated from BMDMs and subjected to RT-PCR. Data were normalized using mouse *GAPDH* as a control gene. For TGFβ and IL10 ELISAs, culture supernatants were collected 12 h after infection; for IL12A and IL27A ELISAs, 48-h postinfection supernatants were collected. *FC*, fold change. Each experimental set is representative of three samples, and error bars are mean ± S.D. Statistical significance was analyzed using one-way analysis of variance followed by Dunnett's multiple comparison test. **, $p < 0.01$; ***, $p < 0.001$.

gradient analysis using 10–40% Ficoll gradients (Fig. S3*A*). Phase-contrast microscopy showed that >60% of metacyclics were present in 6–9-day stationary-phase promastigotes of WT, *LdHSP78+/−*, and resKO parasites (Fig. S3*B*). RT-PCR expression of the *L. donovani SHERPIN* gene revealed comparable amounts of successful metacyclic formation (Fig. S3*C*). Thus, we ensured that all of the following infections were carried out with stationary-phase metacyclic parasites only.

To understand the role of LdHSP78 in animal infection, we first assessed the pathophysiological symptoms of the hamsters infected with three different groups of parasites, up to 3 months postinfection. Similar to infected humans, VL, WT, and resKO parasite-infected hamsters exhibited progressive splenomegaly and hepatomegaly, with high amastigote burdens in organ smears (Fig. 4*A* and Table S2). In *LdHSP78+/−* parasite-infected hamsters, splenic and hepatic lesion formation was delayed significantly, with lower amastigote burdens in spleen and liver stamp smears (Fig. 4*A* and Table S2). Leishman Donovan unit data indicated that infection with WT and resKO parasites resulted in almost 20-fold greater splenic macrophage parasite loads and 25-fold greater hepatic macrophage parasite loads, compared with *LdHSP78+/−* parasite infection (Fig. 4*B*). Since detection of live parasites in the organs provides a better depiction of disease severity and the virulence of parasites, limiting dilution assays (LDAs) with 1 mg/ml minced spleen and liver tissues were performed for animals infected with three different cell lines. LDA data indicated severe declines in parasite burdens, from 10^{10} WT parasites to 10^{3} *LdHSP78+/−* parasites in spleen and from 10^{15} WT parasites to 10^{4} *LdHSP78+/−* parasites in liver 12 weeks postinfection (Fig. 4*C*). Interestingly, in resKO parasite-infected animals, there was almost complete restoration of LDA results in both spleen and liver, indicating that *LdHSP78* overexpression restored virulence of the *LdHSP78+/−* parasites significantly (Fig. 4*C*).

Decreased fitness of *LdHSP78+/−* parasites within hamsters could be confirmed by highly sensitive kinetoplastidial DNA (kDNA)-dependent determination of parasite counts in peripheral blood, spleen, and liver. Parasites were serially diluted from 10^{5} parasites/ml to 1 parasite/ml, and a kDNA standard curve was prepared following a method mentioned elsewhere (Fig. 4*D*) (16). Genomic DNA isolated from hamster peripheral blood, spleen, and liver were then subjected to RT-PCR for kDNA amplification. Based on kDNA C_t values obtained from organs, almost 10 ± 2 parasites/ml WT parasites, 2 ± 1 parasites/ml *LdHSP78+/−* parasites, and 15 ± 2 parasites/ml resKO parasites in animal blood were obtained (Fig. 4*E*). Moreover, parasite loads in *LdHSP78+/−* parasite-infected organs were much lower than those in WT and resKO parasite-infected animals (Fig. 4*E* and Table S3). Subsequently, RT-PCR data for *LdHSP78* mRNA from blood and organs of WT, *LdHSP78+/−*, and resKO parasite-infected animals depicted almost 5-fold (in blood), 10-fold (in spleen), and 4.5-fold (in liver) reductions during *LdHSP78+/−* parasite infection, compared with WT and resKO parasite infections (Fig. 4*F*). The fold changes indicated that the proliferation rate of parasites was significantly compromised in hamsters after partial deletion of *LdHSP78*.

Protective cytokines were enriched during LdHSP78+/− parasite infections

Establishment of VL in hamsters largely depends on the fine balance between Th1 and Th2 responses in spleen (17).

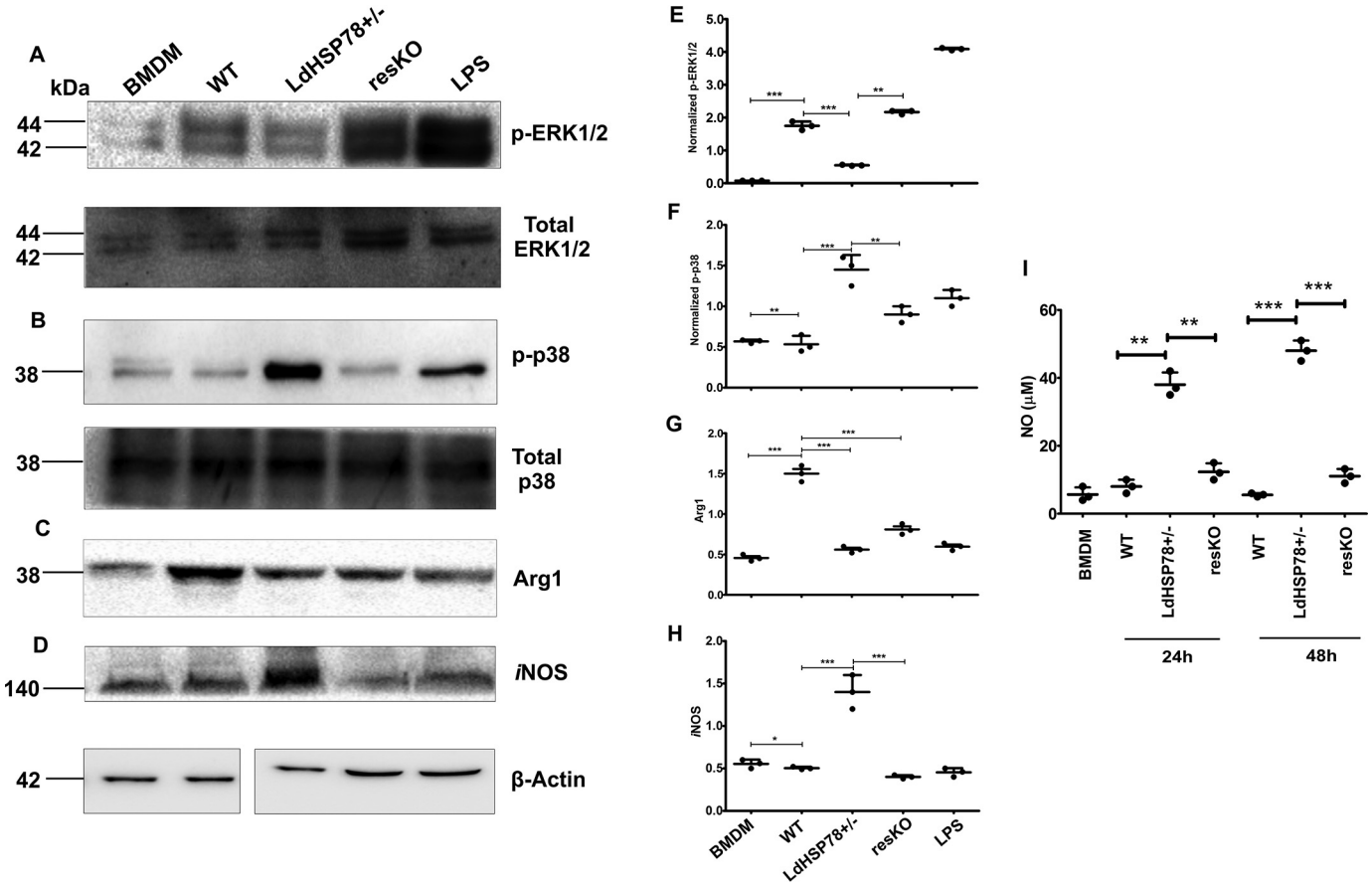

Figure 3. Expression of phospho-p38, iNOS, and NO increased during *LdHSP78*+/− parasite infection in BMDMs. *A–H*, lysates were collected from BMDMs infected for 24 h with WT, LdHSP78+/−, and resKO parasites and Western blotted for phospho-ERK1/2 and total ERK1/2 (phospho-ERK1/2 bands were normalized to ERK1/2 bands) (*A* and *E*), phospho-p38 and total p38 (phospho-p38 bands were normalized to p38 bands) (*B* and *F*), arginase 1 (*Arg1*) (*C* and *G*), and iNOS (*D* and *H*) (arginase 1 and iNOS bands were normalized to β-actin bands). Lipopolysaccharide (LPS) (10 μg/ml) was the positive control and mouse β-actin was the loading control. Scattered plots adjacent to each blot represented mean densitometric values of three blots performed for each protein. *I*, the Griess assay was performed with culture supernatants of WT, *LdHSP78*+/−, and resKO parasite-infected BMDMs collected 24 and 48 h postinfection. Each experimental set is representative of three samples, and error bars are mean ± S.D. Statistical significance was analyzed using one-way analysis of variance followed by Dunnett's multiple-comparison test. *, $p < 0.05$; **, $p < 0.01$; ***, $p < 0.001$.

L. donovani parasites cause enrichment of the immunosuppressive cytokines like IL10 and TGFβ, which supports parasite persistence, whereas parasite clearance is triggered by enrichment of IL12 and IFNγ (17, 18). Findings shown in Fig. 4 suggested that partial deletion of *LdHSP78* triggered rapid clearance of mutant parasites in hamsters. Therefore, fold changes in regulatory cytokine mRNA expression in infected hamster blood, spleen, and liver were compared. As indicated by RT-PCR, IL10 and TGFβ were depleted 12 weeks postinfection (Fig. 5, *A* and *B*), whereas IFNγ was significantly enriched (Fig. 5*C*), in blood, liver, and spleen of *LdHSP78*+/− parasite-infected animals. Cytokine ELISAs also indicated that IL10 titers were exhausted and IL12 was enriched in *LdHSP78*+/− parasite-infected hamsters, which was completely reversed with resKO parasite infection (Fig. 5, *D* and *E*). These findings indicated that, due to enrichment of protective cytokines, *LdHSP78*+/− parasites were unable to establish infections in hamster organs.

NO triggered LdHSP78+/− parasites clearance from hamsters

Earlier, we demonstrated that, after genetic depletion of LdHSP78, clearance of *L. donovani* amastigotes was instigated by macrophage NO (Fig. 3*I*). Therefore, fold changes in iNOS mRNA in blood, spleen, and liver of infected hamsters were studied, which suggested that iNOS expression was higher in *LdHSP78*+/− parasite-infected hamsters, compared with WT and resKO parasite-infected hamsters (Fig. 5*F*). Subsequently, the Griess assay demonstrated time-dependent enrichment of NO in sera of *LdHSP78*+/− parasite-infected animals, compared with their virulent and rescued parasite-infected counterparts (Fig. 5*G*). These studies indicated that, in *in vivo* systems, greater NO enrichment perhaps leads to abrogation of infection in *LdHSP78*+/− parasite-infected hamsters, compared with WT and resKO parasite infections.

Sequence and structural analysis revealed highly conserved NBDs and Clp domain in LdHSP78

Phylogenetic analysis shows wide representation of the HSP78 protein across various phyla (Fig. S4). The 3D model of the *L. donovani* HSP78 protein was generated via MODELLER v9.836 (19), with the coordinates of the ClpB protein from *Thermus thermophilus* (PDB code 1QVR) being used as a potential template. The 3D model was validated using PROCHECK (20) and Verify 3D (21) structure validation tools

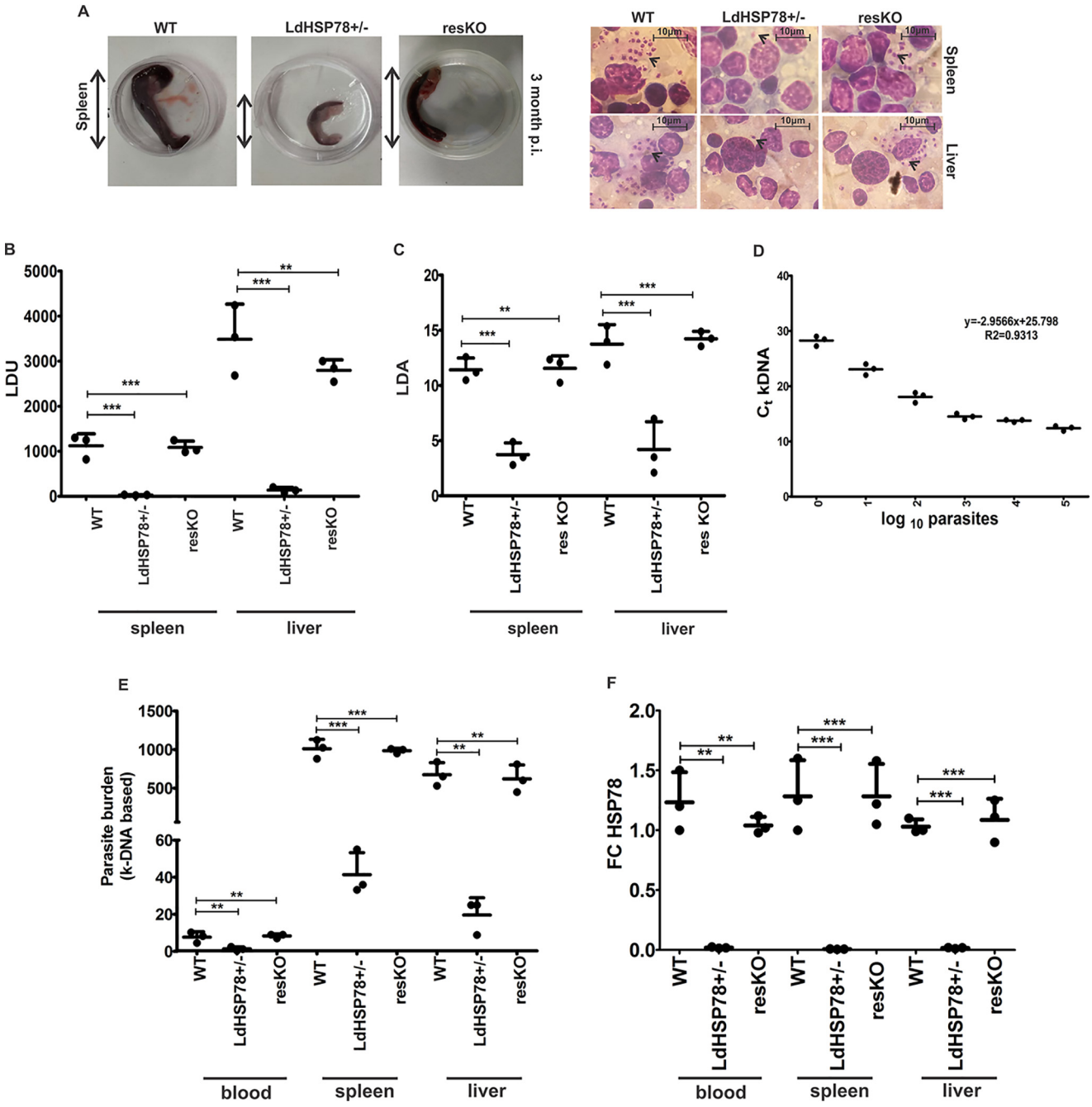

Figure 4. *LdHSP78*+/− parasites showed compromised infectivity in hamsters. *A*, comparative pathophysiology of WT, *LdHSP78*+/−, and resKO parasite-infected spleens procured from hamsters 3 months postinfection (*p.i.*), showing splenomegaly during WT and resKO parasite infection. *B*, Leishman-Donovan units (LDU) from phase-contrast microscopy of Giemsa-stained images (*scale bar*, 10 μm). *C*, LDA results ($\log_{10}$ parasite numbers/ml) for WT, *LdHSP78*+/−, and resKO parasite-infected spleen and liver. *D*, genomic DNA isolated from WT parasites was serially diluted, and RT-PCR for kDNA and *L. donovani GAPDH* was performed. C_t values obtained were used to prepare the standard curve of kDNA *versus* parasite count in $\log_{10}$ count/ml. *E*, C_t values of kDNA from hamster whole blood, spleen, and liver were obtained and plotted in the standard curve of kDNA to calculate the parasite burden of each organ, and results were plotted in this scatter graph. *F*, RT-PCR of *LdHSP78* mRNA from infected hamster organs and whole blood was performed. *FC*, fold change. Each experimental set is representative of three samples, and error bars are mean ± S.D. Statistical significance was analyzed using one-way analysis of variance followed by Dunnett's multiple-comparison test. **, $p < 0.01$; ***, $p < 0.001$.

(Fig. S5). *L. donovani* HSP78 protein can be distinguished into five domains, *e.g.* N-terminal domain (positions 1–136), D1 large domain or NBD1 (positions 151–331), D1 small domain (positions 332–535) containing the ClpB linker, D2 large domain or NBD2 (positions 545–756), and D2 small domain (positions 757–817). NBD1 and NBD2 are relatively more conserved than other domains (Fig. 6*A*) across all phyla. However, ranges of conservation for all five domains are similar in all phyla, as well as in Euglenozoa (contains the Kinetoplastida class) and Ascomycota, the other largest phylum where HSP78 is present (Fig. 6*A*). The N-terminal domain of HSP78 is found to be mostly α-helical, with parallel β-strands inserted near its N terminus. The N-terminal domain is connected to NBD1 through a flexible linker (positions 137–150). The D1 domain is

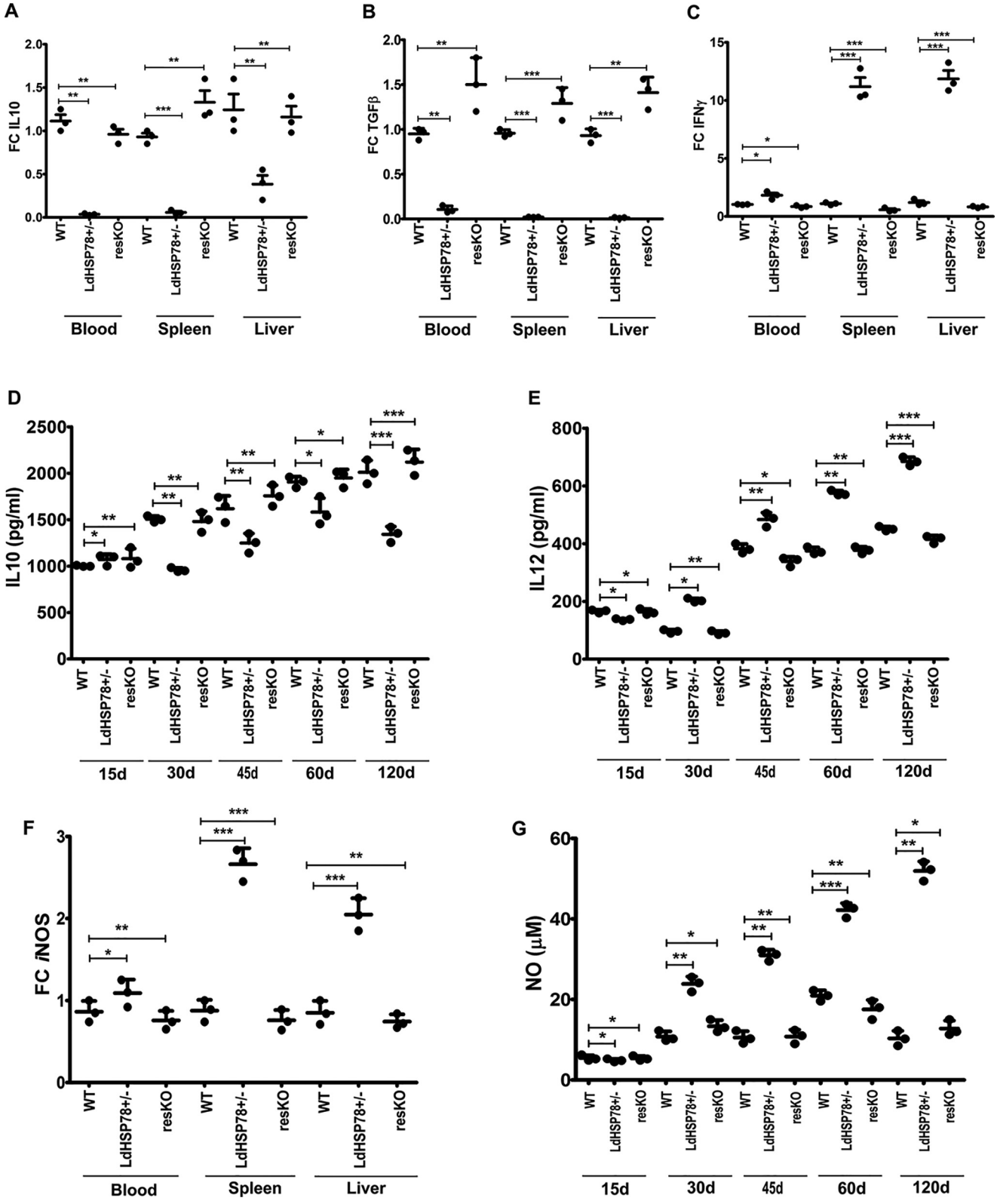

Figure 5. Protective cytokine responses and NO generation were augmented in *LdHSP78*+/− parasite-infected hamsters. *A–C*, IL10 (*A*), TGFβ (*B*), and IFNγ (*C*) levels in whole blood, spleen, and liver of WT, *LdHSP78*+/−, and resKO parasite-infected hamsters from three groups were measured by RT-PCR. *D* and *E*, sandwich ELISAs for IL10 (*D*) and IL12 (*E*) were performed with blood samples collected at regular time intervals up to 3 months. *F* and *G*, enrichment of iNOS (*F*) and NO (*G*) in whole blood, liver, and spleen of hamsters was determined by RT-PCR and Griess assays, respectively. Hamster *GAPDH* was used as the control for all RT-PCR assays. *FC*, fold change. Each experimental set is representative of three animals, and error bars are mean ± S.D. Statistical significance was analyzed using one-way analysis of variance followed by Dunnett's multiple-comparison test. *, $p < 0.05$, **, $p < 0.01$; ***, $p < 0.001$.

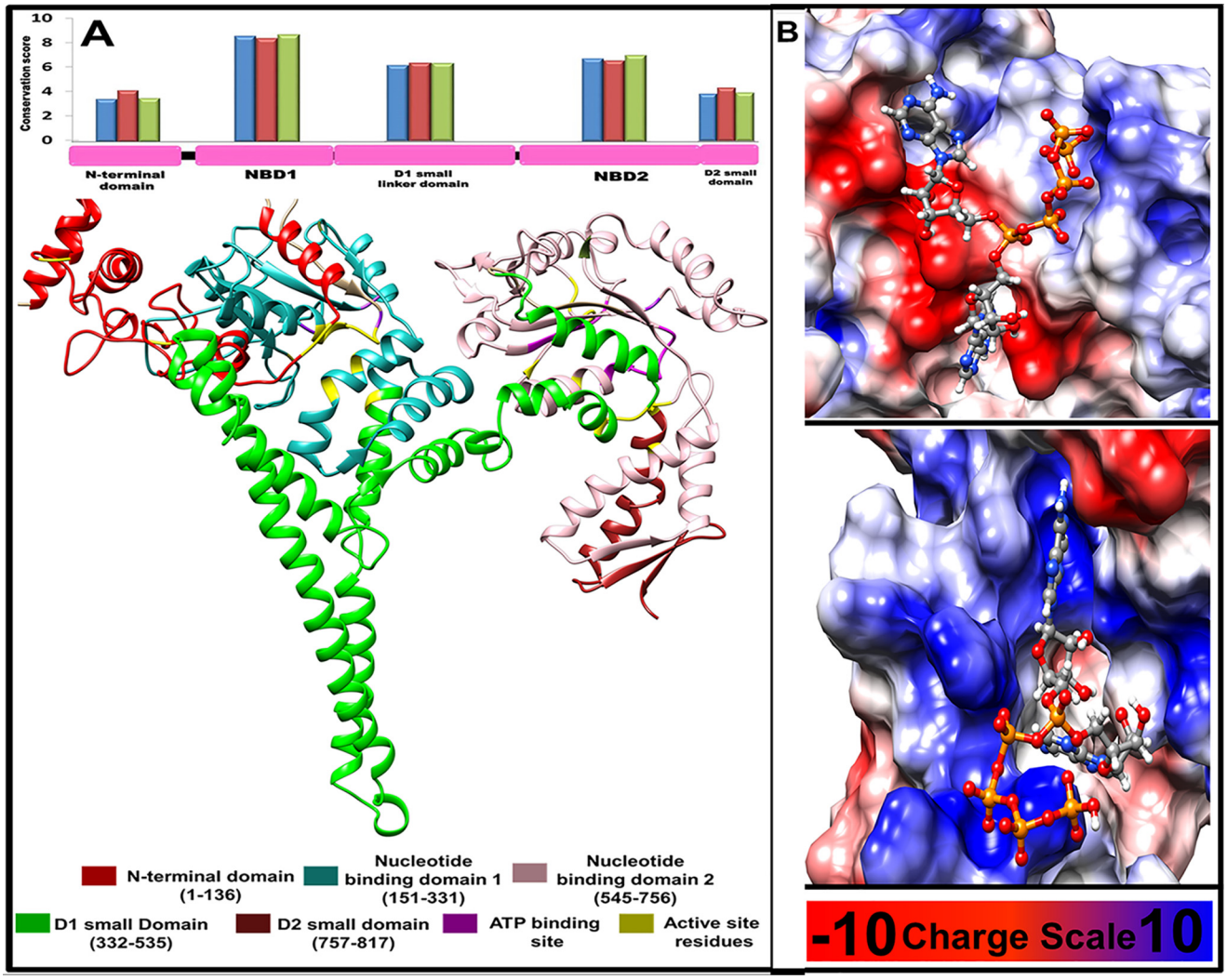

Figure 6. Structural features of *L. donovani* HSP78 protein. *A*, 2D and 3D domain organizations of *L. donovani* HSP78 protein and their relative conservation. *Blue*, *red*, and *green bars* show conservation of individual domain calculated using the representative sequences from all phyla, Euglenozoa, and Ascomycota, respectively. *B*, binding mode and probable interactions of the selected inhibitor Ap5A, which shows significant binding potential for NBD1 and NBD2 shown in upper and lower panel, respectively.

composed of a set of α-helices along with short β-strands and a long coiled coil structure. The coiled coil structure is known as the ClpB linker, containing two short coiled coil motifs. The C-terminal D2 small domain is a mixed α/β structure and lacks the long coiled coil insertion (Fig. 6*A*).

High-throughput virtual screening identified the ATP analog Ap5A as a probable LdHSP78 chemical inhibitor

The high-throughput virtual screening (HTVS) technique was implemented based on two aspects, *de novo* and substrate analog-based screening. Both *de novo* screening and substrate (ATP) analog-based HTVS techniques were applied using the first conformer of 2,838,166 compounds available in the Phase database (22) and 9998 compounds in the PubChem database (23), respectively. Compounds were docked at the nucleotide-binding sites using virtual screening techniques incorporated in the GLIDE package from the Schrodinger suite (24). The molecules that passed the filtration criteria (1460 and 1409 among Phase molecules and 9480 and 9480 among PubChem molecules binding at NBD1 and NBD2, respectively) were further considered for docking with the GOLD program (25), using GOLD fitness scores. Docking complexes possessing similar modes of binding (root mean square deviation of $\leq$5Å) among the top 30% solutions were considered probable inhibitors. This screening yielded 33 and 14 probable molecules binding at NBD1 and NBD2, respectively, whereas substrate analog-based screening suggested 3 and 45 molecules as NBD1 and NBD2 binders, respectively (Fig. S6). Furthermore, a third set of probable inhibitors that are likely to bind both of the NBDs were identified for both *de novo* and analog-based screening methods after comparison of the top 100 GLIDE docking solutions.

Inhibitors bound at NBD1 and NBD2 primarily interacted with 44 and 19 unique HSP78 residues via 66.4% and 60.4% hydrogen bonding, 12.1% and 16.5% electrostatic bonding, 11.2% and 5.2% salt bridge interactions, and 10.2% and 17.9% hydrophobic interactions, respectively (Fig. S7). Ap5A displayed the best docking properties and capability of binding to both of the NBD pockets. Fig. 6*B* shows the mode of interaction of Ap5A binding to NBD1 and NBD2.

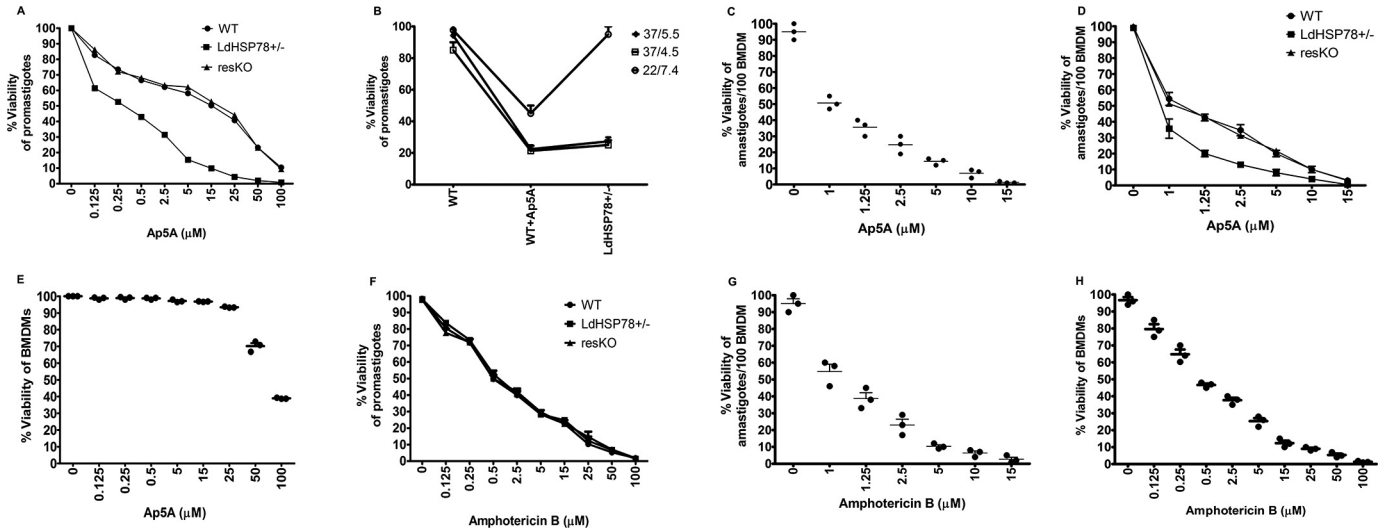

Figure 7. Ap5A showed comparable antileishmanial efficacy with AmB. *A*, *E*, *F*, and *H*, the viability of axenic promastigotes (*A* and *F*) and healthy BMDMs (*E* and *H*) treated with Ap5A and AmB was evaluated using the 3-(4,5-dimethylthiazol-2-yl)-2,5-diphenyltetrazolium bromide reduction assay. *B*, pH sensitivity and temperature sensitivity of Ap5A (15 μM)-treated WT and *LdHSP78*+/− promastigotes were compared by determination of promastigote growth. *C* and *G*, Giemsa staining was performed to calculate the amastigote burden of BMDMs, infected with *L. donovani* for 24 h and treated with either Ap5A or AmB. *A* and *D*, the comparative sensitivity of WT, *LdHSP78*+/−, and resKO promastigotes and amastigotes for Ap5A treatment was analyzed to understand the specificity of Ap5A for LdHSP78. Each experimental set is representative of three samples, and error bars are mean ± S.D. Statistical significance was analyzed using one-way analysis of variance followed by Dunnett's multiple-comparison test.

Chemical inhibition of LdHSP78 by Ap5A resulted in reduced infectivity index of L. donovani in BMDMs

The cytotoxicity of Ap5A ammonium salt was assessed in WT, *LdHSP78*+/−, and resKO promastigote cell lines using the 3-(4,5-dimethylthiazol-2-yl)-2,5-diphenyltetrazolium bromide (MTT) reduction assay. It was observed that the IC_{50} of Ap5A was 14.5 ± 1.92 μM for WT parasites. Ap5A is a structural analog of ATP. Parasites are enriched with multiple ATP-dependent proteins that are as crucial as LdHSP78 for survival; therefore, Ap5A might exert nonspecific effects on the promastigotes. Interestingly, *LdHSP78*+/− parasites exhibited higher sensitivity to Ap5A treatment (IC_{50} = 0.25 ± 0.077 μM), and resKO cell lines (with overexpression of LdHSP78) regained resistance against Ap5A, with an IC_{50} equivalent to that of WT parasites (IC_{50} = 15.0 ± 0.90 μM) (Fig. 7*A*). To further emphasize the specificity of Ap5A for LdHSP78, we compared the growth responses of heterozygous knockouts (*LdHSP78*+/−) and Ap5A-treated WT promastigotes under pH- and temperature-stressed conditions. Ap5A treatment closely mimicked the growth pattern of the promastigotes with partial depletion of LdHSP78. Inhibitor treatment enhanced the sensitivity of WT promastigotes to physiological stresses, similar to that of the *LdHSP78*+/− phenotype (Fig. 7*B*). These findings cumulatively indicated that Ap5A is probably specific for LdHSP78 in the promastigotes.

Infected macrophages were treated for 1 h with vehicle control (20 mM PBS) and a range of Ap5A doses from 1 μM to 15 μM, and cells were kept for 24 h after drug removal in order to understand the leishmanicidal efficacy of Ap5A on amastigotes in BMDMs. The infectivity index calculated by Giemsa staining suggested that the IC_{50} dose of Ap5A for amastigotes was 0.8 ± 0.18 μM (Fig. 7*C*). Furthermore, the sensitivity of WT, *LdHSP78*+/−, and resKO amastigotes to Ap5A was determined to nullify the nonspecific effect of Ap5A on the amastigotes. The IC_{50} of Ap5A for WT amastigotes was 1.00 ± 0.24 μM and that for *LdHSP78*+/− amastigotes was 0.7 ± 0.15 μM. Similar to resKO promastigotes, overexpression of *LdHSP78* led to regained resistance of resKO amastigotes to Ap5A (IC_{50} = 1.2 ± 0.14 μM) (Fig. 7*D*). Thus, the sensitivity of amastigotes to Ap5A also suggested that Ap5A might have specific effects on LdHSP78. However, the IC_{50} of Ap5A for healthy BMDMs was 90 ± 1.55 μM, which was indicative of its poor toxicity against host cells (Fig. 7*E*).

IC_{50} and selective inhibitory (SI) values of Ap5A were compared with those of AmB to understand the efficacy of Ap5A as a potent antileishmanial agent. Therefore, similar experiments were carried out using AmB, which showed that all three promastigote cell lines have almost equivalent sensitivities, *i.e.* the IC_{50} for WT promastigotes is 0.5 ± 0.12 μM, that for *LdHSP78*+/− promastigotes is 0.45 ± 0.13 μM, and that for resKO promastigotes is 0.56 ± 0.07 μM (Fig. 7*F*). Although AmB has a much lower IC_{50} for promastigotes (0.5 ± 0.12 μM), the IC_{50} for amastigotes (1.25 ± 0.59 μM) is very similar to or slightly higher than that of Ap5A (Fig. 7*G*). Nevertheless, the cytotoxicity of AmB for healthy BMDMs is much higher, and the corresponding IC_{50} (0.4 ± 0.19 μM) overlaps with its promastigote and amastigote IC_{50} values (Fig. 7*H*), which further indicated that AmB harms the host cells at a much lower concentration than the concentration at which it kills the parasites. Comparison of SI values for two different inhibitors were undertaken using the World Health Organization guidelines (SI = IC_{50} for BMDMs/IC_{50} for amastigotes). The SI value of Ap5A was 112.5, and the SI value for AmB was 0.8. These data suggested that Ap5A might have promising target-specific antileishmanial efficacy, compared with AmB.

Discussion

Our study identified LdHSP78, a putative AAA+ domain-containing ClpB family member, as a potential virulence factor

of the parasite and explored its role as a therapeutic target. We recognized that LdHSP78 is enriched in VL patient blood and infected hamster organs. To confirm the essentiality of HSP78 in virulence, heterozygous HSP78 knockout parasites of two different species of *Leishmania* were generated by employing conventional homologous recombination-mediated and advanced CRISPR-Cas9-mediated genetic manipulation tools. Null mutation of *LmHSP78*/*LdHSP78* was found to be lethal, and heterozygous mutants had significantly compromised virulence in both *in vitro* and *in vivo* infection models. Interestingly, *LdHSP78*+/− parasites regained their virulence phenotype upon successful add-back of the deleted HSP78 allele in the form of episome. Partial deletion of *LdHSP78* culminated in the inability of the parasites to bypass most of the activated immune responses of the host. Mechanistic understanding of *LdHSP78*+/− parasite clearance suggested that enrichment of phospho-p38 and proinflammatory cytokines preceded activation of NO, which possibly led to *LdHSP78*+/− clearance from macrophages. Thus, after ensuring the essential role of LdHSP78 during infection, we identified Ap5A, an ATP analog, as a potential inhibitor of LdHSP78 and studied its *in vitro* antileishmanial efficacy. We found that Ap5A could successfully clear the parasite load at almost the same dose as AmB in BMDMs but showed greatly reduced toxicity to healthy host macrophages, which is a major hurdle in using AmB.

VL is one of the major global threats next to malaria, causing an estimated 0.5 million new cases annually (WHO reports, 2018) (42, 43). Under such circumstances, VL therapeutics call for urgent identification of novel parasite target proteins that are amenable to high-throughput screening and design of druggable chemical products. In this postgenomic era, integrative computational approaches facilitate the identification and prioritization of candidate targets (26). LdHSP78 is highly conserved in trypanosomes, with no human orthologs, and belongs to the AAA+ superfamily of ATP-dependent HSPs, which efficiently relieves microorganisms from apoptotic shock generated by disaggregated proteins (27). *L. donovani* promastigotes initiate infection by transdifferentiating into amastigotes in the presence of high temperatures and extremely acidic pH (phagosomal pH) inside mammalian macrophages, which is a rate-limiting step for infection initiation. Parasite HSPs play very crucial roles for overriding the stresses induced during this stage (28, 29). Previously, functional significance of HSP83, HSP90, and HSP23 in stress regulation of *Leishmania* was reported (28, 30, 31). However, the prominence of an HSP belonging to the ClpB group as a potential drug target in *L. donovani* has not been explored. Enrichment of LdHSP78 in *L. donovani*-infected BMDMs, hamster organs, and VL patients reinforced its association with active VL.

Clp proteins are reportedly essential for virulence and the persistence of intracellular pathogens such as *Listeria monocytogenes*, *Francisella tularensis*, and *Toxoplasma gondii* inside host macrophages. Therefore, we verified the essentiality of LdHSP78 for the persistence of *L. donovani* inside macrophages by generating HSP78 knockout parasites and then rescued the phenotype using episomal overexpression of HSP78. Significant reduction in *LdHSP78*+/− parasite burdens in BMDMs, paralleled by reduced abundance of *LdHSP78* mRNA expression in amastigotes, indicated LdHSP78 as one of the factors for survival of amastigotes in macrophages.

However, all of our attempts to generate chromosomal null mutants of HSP78 in both *L. donovani* and *L. mexicana* cells, using different genetic manipulation tools, failed. Null mutant parasites survived only in the presence of the episomal vector pXG-GFP expressing HSP78, which was stably maintained even after removal of selection. These findings indicated probable essentiality of the HSP78 gene for promastigote survival, which needs more experimental investigation for confirmation.

Hubel *et al.* reported that HSP100 depletion greatly affects the amastigote stage of development of *L. major* within macrophages (6). We obtained profound LdHSP78 enrichment especially at pH 5.5 and 37 °C. It was interesting that only pH or temperature stress was unable to induce the enrichment but dual stress (both high temperature and low pH), which mimics the macrophage microenvironment, induced LdHSP78 enrichment. Moreover, *LdHSP78*+/− parasites showed impaired growth rates under similar conditions, which indicates that LdHSP78 plays a crucial role as a chaperone during the amastigote stage of development.

To confirm a parasite protein as a potential drug target, it is essential to understand whether knockout parasites are able to survive inside the host and to bypass host defense machineries. Establishment of infection in macrophages is reflected by the cytokine profile. *L. donovani* induces anti-inflammatory cytokines and exhausts proinflammatory cytokine levels in a MAPK-dependent manner, which finally leads to transcription of arginase 1 and suppression of iNOS, aiding survival of the parasites in macrophages (32–36). Proinflammatory cytokines like IL12A were enriched during *LdHSP78*+/− parasite infection. In addition, enhanced phosphorylation of p38 MAPK and up-regulation of iNOS clearly indicated that macrophages are capable of showing active immune responses against *LdHSP78*+/− parasites. For persistence within macrophages, virulent *L. donovani* inhibits iNOS synthesis to be shielded from NO-mediated toxicity (33, 37). In agreement with enriched iNOS expression, NO synthesis was augmented during *LdHSP78*+/− parasite infection, compared with WT parasite infection. Down-regulation of NO was regained after introduction of the *LdHSP78* allele in *LdHSP78*+/− parasites. These studies cumulatively indicated that HSP78 depletion facilitates nonviability of parasites in macrophages in a NO-dependent manner.

Before identification of a potential inhibitor, the role of LdHSP78 in hamster VL was also studied. Comparative infectivity analysis of WT, *LdHSP78*+/−, and resKO parasites in hamsters indicated that heterozygous knockout of *LdHSP78* greatly reduced the capacity of the parasites to proliferate within the infection foci of the animals, such as spleen, liver, and peripheral blood. Besides the decrease in parasite burden and recovery in pathological symptoms of infection, proinflammatory cytokines were enriched and NO titers were increased in *LdHSP78*+/− parasite-infected animals, indicating that the partial depletion of HSP78 disables the parasites from establishing full-grown infections in hamsters. This motivated us to screen for potential HSP78 inhibitor molecules using the HTVS method and to test their antileishmanial efficacies.

It is worth mentioning that ATP analogs represent a novel as well as wide repertoire of pharmacological inhibitors for different diseases, such as cancer, pathological calcification, and multiple myeloma (38–41). *In silico* analysis revealed HSP78 as a putative ATP-dependent HSP; thereafter, by HTVS we screened Ap5A ammonium salt, which is an ATP analog. In this study, the inhibitory role of Ap5A has been substantiated in *L. donovani* infection. However, detailed structural, functional, and pharmacological aspects of Ap5A and its derivatives will be deciphered in the future. A comparative study of the leishmanicidal efficacy of Ap5A ammonium salt with that of AmB revealed that Ap5A had an IC_{50} for amastigotes of 0.8 μM with an SI value of 112.5, whereas AmB had an IC_{50} for amastigotes of 1.25 μM with an SI value 0.8. This indicates that Ap5A can be a potential alternative for AmB, which shows profound toxic effects on the host. However, in order to find better derivatives of the inhibitor, having cytotoxicity for amastigotes in the nanomolar range, a library of Ap5A derivatives was already generated computationally. From them, 23 novel molecules possessing better docking scores and other relevant druggability parameters were selected to initiate a future novel drug development scheme against LdHSP78 protein (Fig. S8).

The impact of this study could be multifaceted, starting from revealing for the first time the importance of the highly conserved ClpB parasite chaperon as an antileishmanial drug target, followed by screening of potential structural analogs (using the HTVS method) against the protein along with its functional validation. In summary, we established that targeting ATP-dependent LdHSP78 with a pharmacological inhibitor can open a new avenue for therapeutic interventions against VL.

Materials and methods

Ethics statement

All animal experiments were approved by the Animal Ethical Committee (Protocol 147/1999/CPSCEA) of the Indian Institute of Chemical Biology, according to the National Regulatory Guidelines issued by the Committee for the Purpose of Control and Supervision on Experimental Animals, under the Division of Animal Welfare, Ministry of Environment and Forest, Government of India.

For human studies, 4–5-ml venous blood samples were collected in individual heparinized vials from three anonymous patients who were initially diagnosed with VL symptoms, such as prolonged fever, hepatosplenomegaly, and pancytopenia, from Rajendra Memorial Research Institute of Medical Science (Patna, Bihar, India). Moreover, samples were tested to be VL positive by the rK39 strip test. Healthy individual blood samples (similar quantities) were collected from both male and female subjects 23–30 years of age. Written approval was obtained from all participants in their local languages. Human sample-related experiments were approved by the Human Ethics Committee of CSIR-Indian Institute of Chemical Biology, abiding by the Declaration of Helsinki principles.

Heterozygous knockout using the UTR-mediated technique

In order to replace *LdHSP78*, UTR sequences flanking the *HYG* gene were cloned; for genomic add-back of the deleted cassette and generation of resKO parasites, the 2454-bp-long *HSP78* gene was cloned by using appropriate primers (Table S3). Details are given in the supporting information.

CRISPR-Cas9-mediated heterozygous knockout generation

Using CRISPR-Cas9 technology, *LmHSP78* deletion was attempted in axenic T7- and Cas9-positive *Leishmania mexicana* cell lines (designed and generously provided by Prof. Jeremy Mottram, University of York, UK). The detailed protocol is provided in the supporting information. Detailed description of the materials and methods is provided in the supporting information.

Data availability

All data are contained within the manuscript and Supporting material. Additional raw data will be shared on request from the following contact persons, a. Dr. Saikat Chakrabarti (saikat@iicb.res.in) b. Dr. Nahid Ali (nail@iicb.res.in).

Acknowledgments—We thank Oishee Chakrabarti (Saha Institute of Nuclear Physics, Kolkata, India) for her valuable advice at different stages of the study. We thank Stephen Beverley (Washington University School of Medicine), Philip Yates (Oregon Health & Science University), and Jeremy Mottram (University of York) for providing the constructs, T7/Cas9-positive *L. mexicana*, and *E. coli* ccdB Survival-T1R cells. We acknowledge Janmenjoy Midya for assistance in animal maintenance, rearing, and handling. S.D. thanks Sohitri Mukherjee (St. Xavier's College, Kolkata, India) for her contributions in cloning and protein-related experiments. We also acknowledge the central instrumentation facility, CSIR-IICB, and Uday Bandyopadhyay and his laboratory (CSIR-IICB) for cloning-related advice.

Author contributions—S. D., N. A., and S. C. conceptualization; S. D., A. B., M. K., N. A., and S. C. resources; S. D., A. B., M. K., and S. C. data curation; S. D., A. B., M. K., N. A., and S. C. formal analysis; S. D., N. A., and S. C. supervision; S. D., N. A., and S. C. funding acquisition; S. D., A. B., M. K., N. A., and S. C. validation; S. D., A. B., and M. K. investigation; S. D., A. B., M. K., S. A. E., M. A., and N. A. methodology; S. D., A. B., and S. C. writing-original draft; S. D., A. B., M. K., and S. C. writing-review and editing; A. B. and M. K. software; N. A. and S. C. visualization; N. A. and S. C. project administration.

Funding and additional information—S. C. acknowledges CSIR-IICB for infrastructure support, CSIR Network Project BSC-0114, Systems Medicine Cluster Grant GAP357 from the Department of Biotechnology, and High-Risk High-Reward Grant HRR/2016/000093 from the Department of Science and Technology for financial support. N. A. acknowledges the J. C. Bose National Fellowship and UK Research and Innovation via the Global Challenges Research Fund (Grant MR/P027989/1) for financial support.

Conflict of interest—The authors declare that they have no conflicts of interest with the contents of this article.

Abbreviations—The abbreviations used are: HSP, heat shock protein; VL, visceral leishmaniasis; NBD, nucleotide-binding domain;

ClpB, caseinolytic protease B; Ap_5A, P^1,P^5-di(adenosine-5′)-pentaphosphate; TGFβ, transforming growth factor β; MAPK, mitogen-activated protein kinase; ERK1/2, extracellular signal-regulated kinase 1/2; kDNA, kinetoplastidial DNA; HTVS, high-throughput virtual screening; iNOS, inducible nitric oxide synthase; NEO, neomycin; PUR, puromycin; HYG, hygromycin; LDA, limiting dilution assay; SI, selective inhibitory; BMDM, bone marrow-derived macrophage; AmB, amphotericin B .

References

1. Li, Z., and Srivastava, P. (2004) Heat-shock proteins. *Curr. Protoc. Immunol.* Appendix 1 CrossRef
2. Zilberstein, D., and Shapira, M. (1994) The role of pH and temperature in the development of *Leishmania* parasites. *Annu. Rev. Microbiol.* **48,** 449–470 CrossRef Medline
3. Callahan, H. L., Portal, I. F., Bensinger, S. J., and Grogl, M. (1996) *Leishmania* spp: temperature sensitivity of promastigotes in vitro as a model for tropism in vivo. *Exp. Parasitol.* **84,** 400–409 CrossRef Medline
4. Pallavi, R., Roy, N., Nageshan, R. K., Talukdar, P., Pavithra, S. R., Reddy, R., Venketesh, S., Kumar, R., Gupta, A. K., Singh, R. K., Yadav, S. C., and Tatu, U. (2010) Heat shock protein 90 as a drug target against protozoan infections: biochemical characterization of HSP90 from *Plasmodium falciparum* and *Trypanosoma evansi* and evaluation of its inhibitor as a candidate drug. *J. Biol. Chem.* **285,** 37964–37975 CrossRef Medline
5. Lee, S., Sowa, M. E., Choi, J. M., and Tsai, F. T. (2004) The ClpB/Hsp104 molecular chaperone: a protein disaggregating machine. *J. Struct. Biol.* **146,** 99–105 CrossRef Medline
6. Hubel, A., Krobitsch, S., Horauf, A., and Clos, J. (1997) *Leishmania major* Hsp100 is required chiefly in the mammalian stage of the parasite. *Mol. Cell Biol.* **17,** 5987–5995 CrossRef Medline
7. Ponte-Sucre, A., Gamarro, F., Dujardin, J. C., Barrett, M. P., Lopez-Velez, R., Garcia-Hernandez, R., Pountain, A. W., Mwenechanya, R., and Papadopoulou, B. (2017) Drug resistance and treatment failure in leishmaniasis: a 21st century challenge. *PLoS Negl. Trop. Dis.* **11,** e0006052 CrossRef Medline
8. Castro, M. D. M., Cossio, A., Velasco, C., and Osorio, L. (2017) Risk factors for therapeutic failure to meglumine antimoniate and miltefosine in adults and children with cutaneous leishmaniasis in Colombia: a cohort study. *PLoS Negl. Trop. Dis.* **11,** e0005515 CrossRef Medline
9. Leonhardt, S. A., Fearson, K., Danese, P. N., and Mason, T. L. (1993) HSP78 encodes a yeast mitochondrial heat shock protein in the Clp family of ATP-dependent proteases. *Mol. Cell Biol.* **13,** 6304–6313 CrossRef Medline
10. Weibezahn, J., Schlieker, C., Bukau, B., and Mogk, A. (2003) Characterization of a trap mutant of the AAA+ chaperone ClpB. *J. Biol. Chem.* **278,** 32608–32617 CrossRef Medline
11. Schlieker, C., Weibezahn, J., Patzelt, H., Tessarz, P., Strub, C., Zeth, K., Erbse, A., Schneider-Mergener, J., Chin, J. W., Schultz, P. G., Bukau, B., and Mogk, A. (2004) Substrate recognition by the AAA+ chaperone ClpB. *Nat. Struct. Mol. Biol.* **11,** 607–615 CrossRef Medline
12. Chio, C. C., Chang, Y. H., Hsu, Y. W., Chi, K. H., and Lin, W. W. (2004) PKA-dependent activation of PKC, p38 MAPK and IKK in macrophage: implication in the induction of inducible nitric oxide synthase and interleukin-6 by dibutyryl cAMP. *Cell. Signal.* **16,** 565–575 CrossRef Medline
13. Stempin, C. C., Dulgerian, L. R., Garrido, V. V., and Cerban, F. M. (2010) Arginase in parasitic infections: macrophage activation, immunosuppression, and intracellular signals. *J. Biomed. Biotechnol.* **2010,** 683485 CrossRef Medline
14. Melby, P. C., Chandrasekar, B., Zhao, W., and Coe, J. E. (2001) The hamster as a model of human visceral leishmaniasis: progressive disease and impaired generation of nitric oxide in the face of a prominent Th1-like cytokine response. *J. Immunol.* **166,** 1912–1920 CrossRef Medline
15. Loria-Cervera, E. N., and Andrade-Narvaez, F. J. (2014) Animal models for the study of leishmaniasis immunology. *Rev. Inst. Med. Trop. Sao Paulo* **56,** 1–11 CrossRef Medline
16. Bhattacharya, P., Ghosh, S., Ejazi, S. A., Rahaman, M., Pandey, K., Ravi Das, V. N., Das, P., Goswami, R. P., Saha, B., and Ali, N. (2016) Induction of IL-10 and TGFβ from $CD4^+CD25^+FoxP3^+$ T cells correlates with parasite load in Indian kala-azar patients infected with *Leishmania donovani*. *PLoS Negl. Trop. Dis.* **10,** e0004422 CrossRef Medline
17. Medina-Colorado, A. A., Osorio, E. Y., Saldarriaga, O. A., Travi, B. L., Kong, F., Spratt, H., Soong, L., and Melby, P. C. (2017) Splenic $CD4^+$ T cells in progressive visceral leishmaniasis show a mixed effector-regulatory phenotype and impair macrophage effector function through inhibitory receptor expression. *PLoS ONE* **12,** e0169496 CrossRef Medline
18. Asad, M., Sabur, A., Shadab, M., Das, S., Kamran, M., Didwania, N., and Ali, N. (2019) EB1-3 chain of IL-35 along with TGF-β synergistically regulate anti-leishmanial immunity. *Front. Immunol.* **10,** 616 CrossRef Medline
19. Webb, B., and Sali, A. (2016) Comparative protein structure modeling using MODELLER. *Curr. Protoc. Bioinformatics* **54,** 5.6.1–5.6.37. CrossRef
20. Laskowski, R. A., Rullmannn, J. A., MacArthur, M. W., Kaptein, R., and Thornton, J. M. (1996) AQUA and PROCHECK-NMR: programs for checking the quality of protein structures solved by NMR. *J. Biomol. NMR* **8,** 477–486 CrossRef Medline
21. Eisenberg, D., Luthy, R., and Bowie, J. U. (1997) VERIFY3D: assessment of protein models with three-dimensional profiles. *Methods Enzymol.* **277,** 396–404 CrossRef Medline
22. Dixon, S. L., Smondyrev, A. M., and Rao, S. N. (2006) PHASE: a novel approach to pharmacophore modeling and 3D database searching. *Chem. Biol. Drug Des.* **67,** 370–372 CrossRef Medline
23. Kim, S., Thiessen, P. A., Bolton, E. E., Chen, J., Fu, G., Gindulyte, A., Han, L., He, J., He, S., Shoemaker, B. A., Wang, J., Yu, B., Zhang, J., and Bryant, S. H. (2016) PubChem Substance and Compound databases. *Nucleic Acids Res.* **44,** D1202–D1213 CrossRef Medline
24. Friesner, R. A., Banks, J. L., Murphy, R. B., Halgren, T. A., Klicic, J. J., Mainz, D. T., Repasky, M. P., Knoll, E. H., Shelley, M., Perry, J. K., Shaw, D. E., Francis, P., and Shenkin, P. S. (2004) Glide: a new approach for rapid, accurate docking and scoring. 1. Method and assessment of docking accuracy. *J. Med. Chem.* **47,** 1739–1749 CrossRef Medline
25. Jones, G., Willett, P., Glen, R. C., Leach, A. R., and Taylor, R. (1997) Development and validation of a genetic algorithm for flexible docking. *J. Mol. Biol.* **267,** 727–748 CrossRef Medline
26. Sosa, E. J., Burguener, G., Lanzarotti, E., Defelipe, L., Radusky, L., Pardo, A. M., Marti, M., Turjanski, A. G., and Fernandez Do Porto, D. (2018) Target-Pathogen: a structural bioinformatic approach to prioritize drug targets in pathogens. *Nucleic Acids Res.* **46,** D413–D418 CrossRef Medline
27. Neckers, L., and Tatu, U. (2008) Molecular chaperones in pathogen virulence: emerging new targets for therapy. *Cell Host Microbe* **4,** 519–527 CrossRef Medline
28. Hombach, A., Ommen, G., Chrobak, M., and Clos, J. (2013) The Hsp90-Sti1 interaction is critical for *Leishmania donovani* proliferation in both life cycle stages. *Cell. Microbiol.* **15,** 585–600 CrossRef Medline
29. Goulhen, F., Hafezi, A., Uitto, V. J., Hinode, D., Nakamura, R., Grenier, D., and Mayrand, D. (1998) Subcellular localization and cytotoxic activity of the GroEL-like protein isolated from *Actinobacillus actinomycetemcomitans*. *Infect. Immun.* **66,** 5307–5313 CrossRef Medline
30. Hombach, A., Ommen, G., MacDonald, A., and Clos, J. (2014) A small heat shock protein is essential for thermotolerance and intracellular survival of *Leishmania donovani*. *J. Cell Sci.* **127,** 4762–4773 CrossRef Medline
31. Krobitsch, S., and Clos, J. (1999) A novel role for 100 kD heat shock proteins in the parasite *Leishmania donovani*. *Cell Stress Chaperones* **4,** 191–198 CrossRef Medline
32. Ansari, N. A., Kumar, R., Gautam, S., Nylen, S., Singh, O. P., Sundar, S., and Sacks, D. (2011) IL-27 and IL-21 are associated with T cell IL-10 responses in human visceral leishmaniasis. *J. Immunol.* **186,** 3977–3985 CrossRef Medline
33. Saha, S., Mondal, S., Ravindran, R., Bhowmick, S., Modak, D., Mallick, S., Rahman, M., Kar, S., Goswami, R., Guha, S. K., Pramanik, N., Saha, B., and Ali, N. (2007) IL-10- and TGF-β-mediated susceptibility in kala-azar and post-kala-azar dermal leishmaniasis: the significance of amphotericin B in

the control of *Leishmania donovani* infection in India. *J. Immunol.* **179,** 5592–5603 CrossRef Medline

34. Bhattacharya, P., Gupta, G., Majumder, S., Adhikari, A., Banerjee, S., Halder, K., Majumdar, S. B., Ghosh, M., Chaudhuri, S., Roy, S., and Majumdar, S. (2011) Arabinosylated lipoarabinomannan skews Th2 phenotype towards Th1 during *Leishmania* infection by chromatin modification: involvement of MAPK signaling. *PLoS ONE* **6,** e24141 CrossRef Medline
35. Junghae, M., and Raynes, J. G. (2002) Activation of p38 mitogen-activated protein kinase attenuates Leishmania donovani infection in macrophages. *Infect. Immun.* **70,** 5026–5035 CrossRef Medline
36. Chandra, D., and Naik, S. (2008) *Leishmania donovani* infection down-regulates TLR2-stimulated IL-12p40 and activates IL-10 in cells of macrophage/monocytic lineage by modulating MAPK pathways through a contact-dependent mechanism. *Clin. Exp. Immunol.* **154,** 224–234 CrossRef Medline
37. Anderson, C. F., Lira, R., Kamhawi, S., Belkaid, Y., Wynn, T. A., and Sacks, D. (2008) IL-10 and TGF-β control the establishment of persistent and transmissible infections produced by *Leishmania tropica* in C57BL/6 mice. *J. Immunol.* **180,** 4090–4097 CrossRef Medline
38. Lecka, J., Ben-David, G., Simhaev, L., Eliahu, S., Oscar, J., Jr., Luyindula, P., Pelletier, J., Fischer, B., Senderowitz, H., and Sevigny, J. (2013) Nonhydrolyzable ATP analogues as selective inhibitors of human NPP1: a combined computational/experimental study. *J. Med. Chem.* **56,** 8308–8320 CrossRef Medline
39. Monkkonen, H., Kuokkanen, J., Holen, I., Evans, A., Lefley, D. V., Jauhiainen, M., Auriola, S., and Monkkonen, J. (2008) Bisphosphonate-induced ATP analog formation and its effect on inhibition of cancer cell growth. *Anticancer Drugs* **19,** 391–399 CrossRef Medline
40. Samsel, M., and Dzierzbicka, K. (2011) Therapeutic potential of adenosine analogues and conjugates. *Pharmacol. Rep.* **63,** 601–617 CrossRef Medline
41. Krett, N. L., Davies, K. M., Ayres, M., Ma, C., Nabhan, C., Gandhi, V., and Rosen, S. T. (2004) 8-Amino-adenosine is a potential therapeutic agent for multiple myeloma. *Mol. Cancer Ther.* **3,** 1411–1420 Medline
42. World Health Organization (2020) *Leishmaniasis*, Geneva, Switzerland. https://www.who.int/news-room/fact-sheets/detail/leishmaniasis.
43. Singh, O. P., Gedda, M. R., Mudavath, S. L., Srivastava, O. N., and Sundar, S. (2019) Envisioning the Innovations in Nanomedicine to Combat Visceral Leishmaniasis: For Future Theranostic Application. *Nanomedicine (Lond).* **14,** 1911–1927 CrossRef Medline